

Implications of Constraints on Mass Parameters in the Higgs Sector of the Nonlinear Supersymmetric SU(5) Model

Dong Won Lee^(a,b), Bjong Ro Kim^(b,c), Sun Kun Oh^(a,b)

^(a) *Department of Physics, Konkuk University, Seoul 143-701, Korea*

^(b) *CHEP, Kyungpook National University, Daegu 702-701, Korea*

^(c) *III. Physikalisches Institut A, RWTH Aachen
D-52056 Aachen, Germany*

Abstract

The Higgs sector of the minimal nonlinear supersymmetric SU(5) model contains three mass parameters. Although these mass parameters are essentially free at the electroweak scale, they might have particular values if they evolve from a particular constraints at the GUT scale through the RG equations. By assuming a number of simple constraints on these mass parameters at the GUT scale, we obtain their values at the electroweak scale through the RG equations in order to investigate the phenomenological implications. Some of them are found to be consistent with the present experimental data.

1 Introduction

Although most of the popular supersymmetric models are linear ones, it is still an open question whether supersymmetry is realized in nature in linear or nonlinear way [1]. One of us have considered a nonlinear realization of supersymmetry with $SU(2) \times U(1)$ symmetry some years ago [2]. This model requires at least two Higgs doublets and a singlet for its Higgs sector. Thus, at least with respect to the Higgs sector, this nonlinear model may be regarded as an alternative to the linear Next-to Minimal Supersymmetric Standard Model (NMSSM). Analysis of this nonlinear model show that it is consistent with phenomenology [3].

An unfavorable aspect of the NMSSM is that its Higgs sector is larger than the simplest linear supersymmetric model, the well-known Minimal Supersymmetric Standard Model (MSSM), which has just two Higgs doublets. The nonlinear alternative that has the same Higgs sector as the MSSM is the minimal nonlinear supersymmetric $SU(5)$ model [4]. The Higgs potential of the low energy limit of this nonlinear model needs effectively only two Higgs doublets. This model has been investigated in some detail by us [4, 5, 6, 7].

However, this minimal nonlinear supersymmetric $SU(5)$ model has a disadvantage compared to the MSSM. That is, it has one more parameter than the MSSM: The Higgs sector of this nonlinear model at the electroweak scale is determined by two Higgs doublets, and the Higgs potential in terms of these Higgs doublets contains in general three mass parameters. These mass parameters are essentially free at the electroweak scale. They are completely independent. On the other hand, the Higgs sector of the MSSM has just two independent parameters.

Therefore, it is worthwhile to look for arguments which allow us to remove this disadvantage, that is, to reduce the number of independent parameters. One of the possibility is given by the *freedom of fine tuning*, that is, to impose some constraints on the mass parameters at the GUT scale. If they are constrained at the GUT scale, their values at the electroweak scale would no longer be free but determined by the renormalization group (RG) equations that govern their evolutions as functions of energy scale.

In this article, we investigate the phenomenological implications of imposing constraints on the mass parameters in the Higgs potential of the minimal nonlinear supersymmetric $SU(5)$ model. By considering a number of simple constraints, which are in fact analogous to the various constrained versions of the MSSM, we examine the mass of the lightest scalar Higgs boson, as well as other Higgs bosons, and their production cross sections in e^+e^- collisions. We find that some of the constraints yield unphysical results or phenomenologically unacceptable results whereas others give results that are consistent with the present experimental data.

This article is organized as follows: In the next section, we describe the argument for the possibility of imposing constraints on the mass parameters. In Section 3, we review the results of unconstrained Higgs potential. In Section 4, we consider a number of constraints in

the increasing order of complexity. Among them we investigate three particular cases which are phenomenologically interesting. Concluding discussions are given in the last section.

2 The Higgs Potential without Parameters

A peculiar aspect of the minimal nonlinear supersymmetric SU(5) model in its spontaneous symmetry breaking from SU(5) to SU(3)×U(1) is the necessity of *manifold fine tuning* in the following sense: In the conventional SU(5) model the spontaneous symmetry breaking of SU(5) to SU(3)×U(1) is induced by the following vacuum expectation values of the diagonal elements of the adjoint Higgs multiplet H^{24}

$$\langle H^{24} \rangle = V_G \begin{pmatrix} 2 & 0 & 0 & 0 & 0 \\ 0 & 2 & 0 & 0 & 0 \\ 0 & 0 & 2 & 0 & 0 \\ 0 & 0 & 0 & -3 + \epsilon & 0 \\ 0 & 0 & 0 & 0 & -3 + \epsilon \end{pmatrix}, \quad (1)$$

where only one fine tuning parameter, ϵ , is introduced, which is of order 10^{-28} GeV, and V_G is of order 10^{16} GeV.

In case of the minimal nonlinear supersymmetric SU(5) model, one needs to introduce three fine tuning parameters such that the vacuum expectation value of H^{24} is given by

$$\langle H^{24} \rangle = V_G \begin{pmatrix} 2 + \epsilon_1 & 0 & 0 & 0 & 0 \\ 0 & 2 + \epsilon_1 & 0 & 0 & 0 \\ 0 & 0 & 2 + \epsilon_1 & 0 & 0 \\ 0 & 0 & 0 & -3 + \epsilon_2 & 0 \\ 0 & 0 & 0 & 0 & -3 + \epsilon_3 \end{pmatrix}, \quad (2)$$

where all of the three fine tuning parameters ϵ_1 , ϵ_2 , and ϵ_3 are of order 10^{-28} . As they satisfy $3\epsilon_1 + \epsilon_2 + \epsilon_3 = 0$, only two of them are independent. We need fine tune them. In the sense that the minimal nonlinear supersymmetric SU(5) model needs one more free fine tuning parameter than the conventional SU(5) model, it might be said that the former is less natural than the latter, as far as the fine tuning is considered to be unnatural.

However, a remarkable merit of the minimal nonlinear supersymmetric SU(5) model is that there is a theoretically consistent method to break SU(5) to SU(3)×U(1) with no need of fine tuning. Unfortunately, the result of the low energy limit of the minimal nonlinear supersymmetric SU(5) model without fine tuning seems to be incompatible with existing experimental data, which will be discussed shortly.

The Higgs potential of the minimal nonlinear supersymmetric SU(5) model, after the breaking of SU(5) all the way down to SU(3)×U(1), in the low energy limit at the electroweak scale is given at the tree level by [4, 5]

$$\begin{aligned}
V = & \frac{1}{8}(g_1^2 + g_2^2)(|H_1|^2 - |H_2|^2)^2 + \frac{1}{2}g_2^2|H_1^+ H_2|^2 \\
& + \lambda^2(|H_1|^2|H_2|^2 - \frac{1}{5}|H_1^T \epsilon H_2|^2) \\
& + m_1^2|H_1|^2 + m_2^2|H_2|^2 + m_3^2(H_1^T \epsilon H_2 + \text{h.c.}),
\end{aligned} \tag{3}$$

where three mass parameters m_1 , m_2 and m_3 are introduced.

These mass parameters are expressed as $m_i = C_i(V_G - \xi_i)$ ($i = 1, 2, 3$), where ξ_i is of the same order of 10^{16} GeV as V_G , and the dimensionless parameter C_i is of order of unity. Generally, both V_G and ξ_i have to be fine tuned such that the difference $V_G - \xi_i$ should be of order of electroweak scale in order to make the model suitable for the electroweak phenomenology. It turns out in the minimal supersymmetric SU(5) model that one can obtain without fine tuning the mass parameters a theoretically consistent model as a low energy limit by breaking first SU(5) to SU(3)×SU(2)×U(1) and then breaking dynamically SU(3)×SU(2)×U(1) to SU(3)×U(1).

First, the breaking of SU(5) to SU(3)×SU(2)×U(1) can be, as shown in Ref [4], accomplished by the vacuum expectation values of the quintuplets H^5 and \bar{H}^5 as $\langle H^5 \rangle = 0$ and $\langle \bar{H}^5 \rangle = 0$, respectively, and the vacuum expectation value of H^{24} given independently of ϵ_i as

$$\langle H^{24} \rangle = V_G \begin{pmatrix} 2 & 0 & 0 & 0 & 0 \\ 0 & 2 & 0 & 0 & 0 \\ 0 & 0 & 2 & 0 & 0 \\ 0 & 0 & 0 & -3 & 0 \\ 0 & 0 & 0 & 0 & -3 \end{pmatrix}. \tag{4}$$

The extremum conditions with respect to $\langle H^{24} \rangle$, $\langle H^5 \rangle$ and $\langle \bar{H}^5 \rangle$ then imply that the three mass parameters in the above tree-level Higgs potential are all zero: $m_1 = m_2 = m_3 = 0$.

Now, for the Higgs potential with $m_1 = m_2 = m_3 = 0$, if $\lambda = 0$, SU(3)×SU(2)×U(1) is spontaneously broken to SU(3)×U(1) at the tree level. If, on the other hand, $\lambda \neq 0$, it is not possible for SU(3)×SU(2)×U(1) to be spontaneously broken at the tree level but only possible at the one-loop level. The parameters are evolved from the GUT scale to the electroweak scale via the RG equations given in Appendix A. We carry out the calculation in the frame of one-loop effective potential given in Appendix B. The renormalization scale is taken to be between 100 GeV and 500 GeV. It turns out that all loop contributions should be included: b and t quark, gauge bosons, and scalar Higgs bosons, where the masses of b and t quark, and the neutral gauge boson are taken as $m_b = 4.3$ GeV, $m_t = 175$ GeV, and $m_Z = 91.187$ GeV, respectively.

Prior to the extremum conditions with respect to $\langle H_0 \rangle$ and $\langle H_1 \rangle$ are imposed, the Higgs potential has two independent parameters, namely, λ and $\tan \beta = v_2/v_1$. After imposing the two extremum conditions, no free parameters are left in the Higgs potential. Therefore, the Higgs potential contains no parameter; it may be called zero-parameter model. For example the Higgs boson masses are uniquely fixed. For m_{S_1} we obtain 35 GeV.

In order to examine whether it is possible for these Higgs bosons to escape from experimental detection, the production cross sections of S_1 in e^+e^- collisions are calculated. The relevant production channels are

$$\begin{aligned}
\text{(i)} \quad & e^+e^- \rightarrow Z \rightarrow ZS_i \rightarrow \bar{f}fS_i \\
\text{(ii)} \quad & e^+e^- \rightarrow Z \rightarrow \bar{f}f \rightarrow \bar{f}fS_i \\
\text{(iii)} \quad & e^+e^- \rightarrow Z \rightarrow PS_i \rightarrow \bar{f}fS_i \\
\text{(iv)} \quad & e^+e^- \rightarrow \gamma \rightarrow \bar{f}f \rightarrow \bar{f}fS_i.
\end{aligned} \tag{5}$$

For $\sqrt{s} = 92$ GeV, we obtain $\sigma_{S_1} = 7$ pb, which is much larger than 1 pb, the discovery limit of LEP1. Therefore, this zero-parameter model is phenomenologically incompatible with the LEP1 data, although it is theoretically interesting in the sense that no fine tuning is required.

3 Unconstrained Higgs Potential

In this section, we summarize the results of unconstrained Higgs potential, where the three mass parameters may have arbitrary values at the GUT scale, in order to demonstrate the effects of the constraints [5, 6, 7].

The Higgs potential of the minimal nonlinear supersymmetric SU(5) model contains three mass parameters, m_i ($i = 1, 2, 3$). In general, the three mass parameters $m_i = C_i(V_G - \xi_i)$ may take any value between zero and say of order 1000 GeV. If we do not use the *freedom of fine tuning*, the three mass parameters are not constrained. In Ref. [5], the phenomenology of this unconstrained model has been treated at the tree level. In Ref. [6], the analysis has been extended to the one-loop level in the frame of effective potential method, where RG equations have not been used and only top and bottom contributions have been taken into account. In Ref. [7], the RG equations have been derived and numerically solved in the $\overline{\text{DR}}$ scheme. Evolving the parameters of the model from the GUT scale down to the electroweak scale, the allowed regions of the parameters are determined, in particular the quartic coupling constant λ . The mass bounds, corrections to tree-level mass sum rules and productions of the Higgs bosons at e^+e^- colliders are investigated for up to 2000 GeV of c.m. energy [7].

We improve the results of these works by employing the RG equations given in Appendix A and including not only top and bottom contributions but also gauge and Higgs self contributions for the masses and cross sections.

At the GUT scale, we set the values of parameters to be

$$\begin{aligned}
0 &\leq \lambda_{\text{GUT}} \leq 1.2 \\
-1 &\leq m_{i_{\text{GUT}}}^2 \text{ (TeV}^2\text{)} \leq 1 \\
1 &\leq \tan\beta \leq 20,
\end{aligned}
\tag{6}$$

where $i = 1, 2, 3$, and calculate their values at the electroweak scale using the RG equations. At the electroweak scale, we require the square masses of the Higgs bosons to be positive and $\tan\beta$ to be in the range of $1 \leq \tan\beta \leq 20$.

We obtain the following numbers for m_{S_1} , m_{S_2} and m_P , which are respectively the masses of the Higgs scalars S_1, S_2 and pseudoscalar P :

$$\begin{aligned}
31.6 &\leq m_{S_1} \text{ (GeV)} \leq 183.4 \\
114 &\leq m_{S_2} \text{ (GeV)} \leq 1311 \\
24 &\leq m_P \text{ (GeV)} \leq 1311.
\end{aligned}
\tag{7}$$

We calculate the production cross sections for the lightest scalar Higgs boson S_1 in e^+e^- collisions. The relevant channels are the same as eq. (5). As no scalar Higgs boson has discovered at LEP, it might have escaped the detection or its mass is bounded from below. For $\sqrt{s} = 205.9$ GeV, which is the center of mass energy reached finally at LEP2, assuming the discovery limit of 40fb for LEP2, we find that S_1 should be heavier than 66 GeV in order to escape the detection at LEP2.

Future e^+e^- colliders may discover the Higgs bosons of this unconstrained model. Assuming that at least 10 signal events are necessary to detect the Higgs bosons, we set the necessary minimum luminosity L_{min} for given center of mass energy of the future e^+e^- colliders: For the S_1 production, we find that L_{min} is respectively 1.43 fb^{-1} , 5.4 fb^{-1} , and 21.3 fb^{-1} for $\sqrt{s} = 500, 1000$, and 2000 GeV. For the S_2 production, we obtain that $L_{\text{min}} = 23.8 \text{ fb}^{-1}$ for $\sqrt{s} = 2000$ GeV, and for the P production, $L_{\text{min}} = 77 \text{ fb}^{-1}$ for $\sqrt{s} = 2000$ GeV. An integrated luminosity of this order for the future linear collider is sufficiently realistic, as the proposed linear collider project suggests that the baseline luminosity for the $\sqrt{s} = 500$ GeV e^+e^- linear collider is above $10^{34} \text{ cm}^{-2}\text{s}^{-1}$ [8].

4 Constrained Higgs Potential

Now, let us use the *freedom of fine tuning* at the GUT scale. The simplest form of fine tuning the mass parameters would be such that the number of them is reduced. In other words, we eliminate some of the mass parameters by fine tuning them. For example, we may eliminate all of them by tuning $m_{1_{\text{GUT}}}^2 = m_{2_{\text{GUT}}}^2 = m_{3_{\text{GUT}}}^2 = 0$, or two of them by

setting either $m_{1\text{GUT}}^2 = m_{2\text{GUT}}^2 = 0$ but $m_{3\text{GUT}}^2 \neq 0$, $m_{2\text{GUT}}^2 = m_{3\text{GUT}}^2 = 0$ but $m_{1\text{GUT}}^2 \neq 0$, or $m_{1\text{GUT}}^2 = m_{3\text{GUT}}^2 = 0$ but $m_{2\text{GUT}}^2 \neq 0$, and so on. We find that among them, three cases of fine tunings yield phenomenologically reasonable results:

$$\begin{aligned}
& \text{(Case A)} \quad m_{2\text{GUT}}^2 = 0, \quad m_{1\text{GUT}}^2 \neq 0, \quad m_{3\text{GUT}}^2 \neq 0 \\
& \text{(Case B)} \quad m_{1\text{GUT}}^2 = 0, \quad m_{2\text{GUT}}^2 \neq 0, \quad m_{3\text{GUT}}^2 \neq 0 \\
& \text{(Case C)} \quad |m_{1\text{GUT}}^2| = |m_{2\text{GUT}}^2| = |m_{3\text{GUT}}^2| \neq 0.
\end{aligned} \tag{8}$$

We consider these three cases one by one. Note that we take $0 \leq \lambda_{\text{GUT}} \leq 1.2$ at the GUT scale for our analysis and $0 < |m_{i\text{GUT}}^2| \text{ (TeV}^2) \leq 1$ for the mass parameters. The other values we take in our calculations at the electroweak scale are $m_b = 4.3 \text{ GeV}$, $m_t = 175 \text{ GeV}$, and $m_Z = 91.187 \text{ GeV}$, and $1 \leq \tan \beta \leq 20$.

4.1 Two-Parameter Higgs Potential

Case A

In Case A, there are two independent mass parameters. We fine tune at the GUT scale one of the mass parameters to be zero, and let the other two mass parameters vary independently. From the GUT scale where we set $m_{2\text{GUT}}^2 = 0$, $0 < |m_{1\text{GUT}}^2| \text{ (TeV}^2) \leq 1$, $0 < |m_{3\text{GUT}}^2| \text{ (TeV}^2) \leq 1$ and $0 \leq \lambda_{\text{GUT}} \leq 1.2$, the RG equations lead us at the electroweak scale to

$$\begin{aligned}
(107)^2 &\leq m_1^2 \text{ (GeV}^2) \leq (1176)^2 \\
-(133)^2 &\leq m_2^2 \text{ (GeV}^2) \leq -(52)^2 \\
-(272)^2 &\leq m_3^2 \text{ (GeV}^2) \leq -(45.4)^2 \\
0.005 &\leq \lambda \leq 0.388.
\end{aligned} \tag{9}$$

With these allowed parameters, we calculate the Higgs boson masses at the electroweak scale. We plot m_{S_1} in Fig. 1, where one can see that points are scattered between 104.6 GeV and 183.4 GeV for m_{S_1} . In this way, we set the ranges for the Higgs boson masses. The results are:

$$\begin{aligned}
104.6 &\leq m_{S_1} \text{ (GeV)} \leq 183.4 \\
129.4 &\leq m_{S_2} \text{ (GeV)} \leq 1178 \\
156 &\leq m_P \text{ (GeV)} \leq 1178.
\end{aligned} \tag{10}$$

Note that all the Higgs bosons are heavier than the Z boson mass. The allowed range for m_{S_1} is rather tight compared to the allowed ranges for m_{S_2} or m_P .

Now, the cross sections for the productions of these Higgs bosons are calculated in order to check the possibility of detecting these Higgs bosons in e^+e^- collisions. For $\sqrt{s} = 205.9 \text{ GeV}$,

the center of mass energy of LEP2, the results of our calculations show that the production cross sections for all these Higgs bosons are well below the discovery limit of LEP2. Thus, in Case A, the existing experimental data cannot put any constraints on the masses of the three Higgs bosons in the minimal nonlinear supersymmetric SU(5) model.

The cross sections for the productions of these Higgs bosons at the future e^+e^- linear colliders are also calculated. For S_1 , we plot in Fig.2 σ_{S_1} for its production in e^+e^- collisions at $\sqrt{s} = 500$ GeV. One can see that σ_{S_1} lies between about 7 and 9.8 fb. We also calculate for other center of mass energies. Thus, the results for S_1 production in e^+e^- collisions for $\sqrt{s} = 500$ (1000, 2000) GeV are

$$7 (1.85, 0.47) \leq \sigma_{S_1} \text{ (fb)} \leq 9.8 (2.4, 0.5). \quad (11)$$

The lower bounds for σ_{S_2} and σ_P are nearly zero in e^+e^- collisions at $\sqrt{s} = 500$ GeV. This implies that they might not be discovered for some parameter regions of the minimal nonlinear supersymmetric SU(5) model. However, the upper bound for σ_{S_2} and σ_P are comparatively larger than that of σ_{S_1} : Our calculations yield that $\sigma_{S_2} \leq 285.1$ fb and $\sigma_P \leq 284.1$ fb at $\sqrt{s} = 500$ GeV.

In e^+e^- collisions at $\sqrt{s} = 1000$ GeV, both S_2 and P might be produced heftily. The production cross sections for both of them are obtained as

$$0 \leq \sigma_{S_2, P} \text{ (fb)} \leq 320, \quad (12)$$

for $\sqrt{s} = 1000$ GeV. Thus, in Case A, there are some parameter regions in the minimal nonlinear supersymmetric SU(5) model where these Higgs bosons might be produced in large quantity at the future high energy e^+e^- linear colliders.

Extending our analysis for the future e^+e^- linear colliders with $\sqrt{s} = 2000$ GeV, we obtain that, as can be seen in Fig. 3,

$$\begin{aligned} \sigma_{S_2} &\geq 1.9 \text{ fb} \\ \sigma_P &\geq 1.8 \text{ fb}. \end{aligned} \quad (13)$$

Case B

The Case B has also only two free mass parameters at the GUT scale. We set $m_{1\text{GUT}}^2 = 0$, and allow other parameters to take values in the following ranges at the GUT scale:

$$\begin{aligned} 0 &< |m_{2\text{GUT}}^2| \text{ (TeV}^2) &\leq 1 \\ 0 &< |m_{3\text{GUT}}^2| \text{ (TeV}^2) &\leq 1 \\ 0 &\leq \lambda_{\text{GUT}} &\leq 1.2. \end{aligned} \quad (14)$$

Via RG equations, these parameters evolve from the GUT scale down to the electroweak scale to have values as follows:

$$\begin{aligned}
(40.6)^2 &\leq m_1^2 \text{ (GeV}^2) \leq (146.7)^2 \\
-(136.8)^2 &\leq m_2^2 \text{ (GeV}^2) \leq -(61.7)^2 \\
-(94.4)^2 &\leq m_3^2 \text{ (GeV}^2) \leq 0 \\
0.013 &\leq \lambda \leq 0.388.
\end{aligned}
\tag{15}$$

These values for the parameters yield relatively light Higgs bosons. As are illustrated in Fig. 4, Fig. 5 and Fig. 6, respectively, for m_{S_1} , m_{S_2} and m_P , we obtain that

$$\begin{aligned}
31.6 &\leq m_{S_1} \text{ (GeV)} \leq 162 \\
118 &\leq m_{S_2} \text{ (GeV)} \leq 191 \\
25.5 &\leq m_P \text{ (GeV)} \leq 169.
\end{aligned}
\tag{16}$$

With these mass ranges, S_1 and P can be produced in e^+e^- collisions at the center of mass energy of LEP1, whereas S_2 production is not allowed kinematically. However, the production of P is suppressed due to the absence of its Higgs-strahlung process, which is the dominant one for S_1 at the LEP1 energy. So the no detection at LEP1 of S_1 may put a lower bound on m_{S_1} as

$$46 \leq m_{S_1} \text{ (GeV)}. \tag{17}$$

If the e^+e^- center of mass energy is as large as the LEP2, all the three Higgs bosons can be produced. Here, too, the production of P is strongly suppressed by the same reason as given at LEP1. For LEP2 with $\sqrt{s} = 205.9$ GeV we plot σ_{S_1} and σ_{S_2} in Fig. 7. From this figure, assuming the discovery limit of 40 fb for LEP2, one might put a lower bound on the mass of S_1 as $m_{S_1} \geq 67.5$ GeV. On the other hand, one can see that σ_{S_2} is smaller than 2 fb for the entire region of the parameter space, which is well below the discovery limit of LEP2. Thus, LEP2 cannot put any limit on m_{S_2} .

In e^+e^- collisions with very high center of mass energy, the channel (iv) in equation (5) is comparably dominant with other channels in size and σ_P becomes the same order of magnitude as σ_{S_1} and σ_{S_2} . We allow the parameters to vary within the ranges obtained by the RG equations, and calculate the production cross sections. We obtain the following lower bounds for them: For e^+e^- collisions with $\sqrt{s} = 500$ GeV,

$$\begin{aligned}
\sigma_{S_1} &\geq 7 \text{ fb} \\
\sigma_{S_2} &\geq 6.4 \text{ fb} \\
\sigma_P &\geq 2 \text{ fb},
\end{aligned}
\tag{18}$$

for e^+e^- collisions with $\sqrt{s} = 1000$ GeV,

$$\begin{aligned}\sigma_{S_1} &\geq 1.85 \text{ fb} \\ \sigma_{S_2} &\geq 1.5 \text{ fb} \\ \sigma_P &\geq 0.43 \text{ fb},\end{aligned}\tag{19}$$

and for e^+e^- collisions with $\sqrt{s} = 2000$ GeV,

$$\begin{aligned}\sigma_{S_1} &\geq 0.47 \text{ fb} \\ \sigma_{S_2} &\geq 0.42 \text{ fb} \\ \sigma_P &\geq 0.13 \text{ fb}.\end{aligned}\tag{20}$$

4.2 One-Parameter Higgs Potential

Let us consider the Case C. The Higgs potential in the Case C contains only one mass parameter at the GUT scale, namely, $0 < |m_{1\text{GUT}}^2| = |m_{2\text{GUT}}^2| = |m_{3\text{GUT}}^2| \leq 1(\text{TeV}^2)$ and we set $0 \leq \lambda_{\text{GUT}} \leq 1.2$. The RG equations yield their values at the electroweak scale as

$$\begin{aligned}(95)^2 &\leq m_1^2 (\text{GeV}^2) \leq (296.7)^2 \\ -(110.6)^2 &\leq m_2^2 (\text{GeV}^2) \leq -(113)^2 \\ -(214.3)^2 &\leq m_3^2 (\text{GeV}^2) \leq -(56.9)^2 \\ 0.004 &\leq \lambda \leq 0.385.\end{aligned}\tag{21}$$

And these values in turn yield the masses of the Higgs bosons as

$$\begin{aligned}85 &\leq m_{S_1} (\text{GeV}) \leq 173 \\ 141 &\leq m_{S_2} (\text{GeV}) \leq 345 \\ 136 &\leq m_P (\text{GeV}) \leq 336.\end{aligned}\tag{22}$$

Now we calculate σ_{S_1} at the LEP2 energy, $\sqrt{s} = 205.9$ GeV. For given m_{S_1} , we search the entire region of the parameter space and select the largest σ_{S_1} . In Fig. 8, we plot the result as a function of m_{S_1} . Assuming the discovery limit of 40fb for LEP2, Fig. 8 indicates that there are some parameter regions for $m_{S_1} \leq 107.3$ GeV where S_1 might be detected at LEP2. Thus, the figure suggests that the lower bound on the mass of the lightest scalar Higgs boson in our model is set as 107.3 GeV by LEP2.

In the future e^+e^- linear colliders the cross section for the production of the lightest scalar Higgs boson S_1 in this case is

$$7.5 (1.9, 0.48) \leq \sigma_{S_1} (\text{fb}) \leq 12.5 (4.3, 1.18),\tag{23}$$

for $\sqrt{s} = 500$ (1000, 2000) GeV. For other Higgs bosons, we obtain that

$$\begin{aligned} 0 \text{ (1.5, 0.42)} &\leq \sigma_{S_2}(\text{fb}) \leq 80 \text{ (35, 8)} \\ 0 \text{ (1.0, 0.28)} &\leq \sigma_P(\text{fb}) \leq 78 \text{ (35, 8)}, \end{aligned} \tag{24}$$

for $\sqrt{s} = 500$ (1000, 2000) GeV. The tendency is that the cross sections decrease as the Higgs bosons become heavier and the cross sections increase as the Higgs bosons become lighter. For S_2 and P , the minimum cross section for producing them at a $\sqrt{s} = 500$ GeV e^+e^- colliding machine is nearly zero. However, the large upper bounds on the production cross sections suggest that they might also be detected at the future e^+e^- linear colliders depending on their masses.

Note that these numbers are large enough for the future e^+e^- linear colliders to examine the Case C of the minimal nonlinear supersymmetric SU(5) model. Thus, if the discovery limit for the e^+e^- linear colliders at $\sqrt{s} = 500$ GeV is 10 events, one would need an integrated luminosity of at least about 1.33 fb^{-1} . In order to test the model by detecting, for example, S_1 , the minimum cross section of whose production is about 7.5 fb.

5 Discussions and Conclusions

We have investigated if the minimal nonlinear supersymmetric SU(5) model is phenomenologically viable, by fine-tuning the mass parameters of the Higgs potential. We have set some of the mass parameters to be constrained at the GUT scale, and then have evolved them down to the electroweak scale via RG equations. We have found that three cases emerge as acceptable.

One of them is the case where m_2 , the mass term of the Higgs doublet H_2 , which gives mass to the top-quark, is set to be zero at the GUT scale. A characteristic feature of this case is that the mass of the lightest scalar Higgs boson is predicted as $104.6 \leq m_{S_1} \text{ (GeV)} \leq 183.4$. Note that the lower bound of m_{S_1} is rather large while the allowed range of m_{S_1} is comparatively narrow.

Another case is obtained by fine-tuning m_1 , the mass term of the doublet H_1 , which gives mass to the bottom-quark, to be zero at the GUT scale. A novel feature of this case is that all scalar Higgs bosons are predicted to be lighter than 200 GeV.

The other case has only one mass parameter at the GUT scale. It is obtained by fine-tuning $|m_{1\text{GUT}}^2|$, $|m_{2\text{GUT}}^2|$ and $|m_{3\text{GUT}}^2|$ to be equal non-zero value at the GUT scale. In this case, all scalar Higgs bosons are predicted to be between 85 GeV and 345 GeV.

We have also shown that these three cases are compatible with the data of LEP1 and LEP2. We have calculated the lower bounds for the production cross sections of some Higgs bosons at the future e^+e^- colliders with $\sqrt{s} = 500$, 1000, and 2000 GeV. The numbers are within the range of the discovery limit of the future machines, thus allowing our model to be examined.

Appendix A

RG equations of the nonlinear Supersymmetric SU(5) model

The RG equations of the parameters of our model are derived as follows:

$$\begin{aligned} \frac{d\lambda_1}{dt} = & \frac{1}{16\pi^2} \left\{ 12\lambda_1^2 + 4\lambda_3^2 + 4\lambda_3\lambda_4 + 2\lambda_4^2 + 2\lambda_5^2 + 24\lambda_6^2 \right. \\ & - \lambda_1(3g_1^2 + 9g_2^2 - 12h_b^2) + \frac{3}{2}g_2^4 \\ & \left. + \frac{3}{4}(g_1^2 + g_2^2)^2 - 12h_b^4 \right\} \end{aligned}$$

$$\begin{aligned} \frac{d\lambda_2}{dt} = & \frac{1}{16\pi^2} \left\{ 12\lambda_2^2 + 4\lambda_3^2 + 4\lambda_3\lambda_4 + 2\lambda_4^2 + 2\lambda_5^2 + 24\lambda_6^2 \right. \\ & - \lambda_2(3g_1^2 + 9g_2^2 - 12h_t^2) + \frac{3}{2}g_2^4 \\ & \left. + \frac{3}{4}(g_1^2 + g_2^2)^2 - 12h_t^4 \right\} \end{aligned}$$

$$\begin{aligned} \frac{d\lambda_3}{dt} = & \frac{1}{16\pi^2} \left\{ 4\lambda_3^2 + 2\lambda_4^2 + (\lambda_1 + \lambda_2)(6\lambda_3 + 2\lambda_4) \right. \\ & + 2\lambda_5^2 + 4\lambda_6^2 + 4\lambda_7^2 + 16\lambda_6\lambda_7 \\ & - \lambda_3(3g_1^2 + 9g_2^2 - 6h_b^2 - 6h_t^2) \\ & \left. + \frac{9}{4}g_2^4 + \frac{3}{4}g_1^4 - 12h_b^2h_t^2 \right\} \end{aligned}$$

$$\begin{aligned} \frac{d\lambda_4}{dt} = & \frac{1}{16\pi^2} \left\{ 8\lambda_3\lambda_4 + 2\lambda_4(\lambda_1 + \lambda_2) + 4\lambda_4^2 + 8\lambda_5^2 \right. \\ & + 10\lambda_6^2 + 10\lambda_7^2 + 4\lambda_6\lambda_7 \\ & - \lambda_4(3g_1^2 + 9g_2^2 - 6h_b^2 - 6h_t^2) \\ & \left. + 12h_b^2h_t^2 + 3g_1^2g_2^2 \right\} \end{aligned}$$

$$\begin{aligned} \frac{d\lambda_5}{dt} = & \frac{1}{16\pi^2} \left\{ 2\lambda_5(\lambda_1 + \lambda_2 + 4\lambda_3 + 6\lambda_4) + 10(\lambda_6^2 + \lambda_7^2) \right. \\ & \left. + 4\lambda_6\lambda_7 - \frac{1}{2}\lambda_5(18g_2^2 + 6g_1^2 - 12(h_t^2 + h_b^2)) \right\} \end{aligned}$$

$$\begin{aligned} \frac{d\lambda_6}{dt} = & \frac{1}{16\pi^2} \left\{ 2\lambda_6(6\lambda_1 + 3\lambda_3 + 4\lambda_4 + 5\lambda_5) \right. \\ & + 2\lambda_7(3\lambda_3 + 2\lambda_4 + \lambda_5) \\ & \left. - \frac{1}{4}\lambda_6(36g_2^2 + 12g_1^2 - 12(h_t^2 + 3h_b^2)) \right\} \end{aligned}$$

$$\begin{aligned} \frac{d\lambda_7}{dt} = & \frac{1}{16\pi^2} \left\{ 2\lambda_7(6\lambda_2 + 3\lambda_3 + 4\lambda_4 + 5\lambda_5) \right. \\ & + 2\lambda_6(3\lambda_3 + 2\lambda_4 + \lambda_5) \\ & \left. - \frac{1}{4}\lambda_7(36g_2^2 + 12g_1^2 - 12(3h_t^2 + h_b^2)) \right\} \end{aligned}$$

$$\begin{aligned} \frac{d\mu_1^2}{dt} = & \frac{1}{32\pi^2} \left\{ 12\lambda_1\mu_1^2 + (8\lambda_3 + 4\lambda_4)\mu_2^2 \right. \\ & \left. + 24\lambda_6\mu_3^2 - 2(9g_2^2 + 3g_1^2 - 12h_b^2)\mu_1^2 \right\} \end{aligned}$$

$$\begin{aligned}
\frac{d\mu_2^2}{dt} &= \frac{1}{32\pi^2} \left\{ 12\lambda_2\mu_2^2 + (8\lambda_3 + 4\lambda_4)\mu_1^2 \right\} \\
&\quad + 24\lambda_7\mu_3^2 - 2(9g_2^2 + 3g_1^2 - 12h_t^2)\mu_2^2 \Big\} \\
\frac{d\mu_3^2}{dt} &= \frac{1}{32\pi^2} \left\{ (4\lambda_3 + 8\lambda_4 + 12\lambda_5)\mu_3^2 + 12\lambda_6\mu_1^2 \right. \\
&\quad \left. + 12\lambda_7\mu_2^2 - (18g_2^2 + 6g_1^2 - 12h_b^2 - 12h_t^2)\mu_3^2 \right\} \\
\frac{dh_t}{dt} &= -\frac{h_t}{16\pi^2} \left(8g_3^2 + \frac{9}{4}g_2^2 + \frac{17}{12}g_1^2 - \frac{1}{2}h_b^2 - \frac{9}{2}h_t^2 \right) \\
\frac{dh_b}{dt} &= -\frac{h_b}{16\pi^2} \left(8g_3^2 + \frac{9}{4}g_2^2 + \frac{5}{12}g_1^2 - \frac{1}{2}h_t^2 - \frac{9}{2}h_b^2 \right), \tag{25}
\end{aligned}$$

where the following redefinition of the parameters are used

$$\begin{aligned}
\lambda_1(M_{\text{GUT}}) &= \frac{g_1^2(M_{\text{GUT}}) + g_2^2(M_{\text{GUT}})}{4} \\
\lambda_2(M_{\text{GUT}}) &= \frac{g_1^2(M_{\text{GUT}}) + g_2^2(M_{\text{GUT}})}{4} \\
\lambda_3(M_{\text{GUT}}) &= \frac{g_2^2(M_{\text{GUT}}) - g_1^2(M_{\text{GUT}})}{4} + \lambda^2(M_{\text{GUT}}) \\
\lambda_4(M_{\text{GUT}}) &= -\frac{1}{2}g_2^2(M_{\text{GUT}}) - \frac{1}{5}\lambda^2(M_{\text{GUT}}) \\
\lambda_5(M_{\text{GUT}}) &= \lambda_6(M_{\text{GUT}}) = \lambda_7(M_{\text{GUT}}) = 0 \\
\mu_i^2(M_{\text{GUT}}) &= m_i^2(M_{\text{GUT}}),
\end{aligned}$$

where $i = 1, 2, 3$. Note that μ_1 and μ_2 are eventually eliminated from the potential by the extremum conditions.

From the known values of the gauge couplings at m_Z scale [9] we obtain $g_1^2(m_Z) = 0.1283$, $g_2^2(m_Z) = 0.4273$ and $g_3^2(m_Z) = 1.4912$ in the $\overline{\text{DR}}$ renormalization scheme. Through their RG evolution from m_Z scale to m_t scale with five quarks and one Higgs doublet, the top-quark Yukawa coupling is obtained from $m_t^{\text{pole}} = \frac{1}{\sqrt{2}}h_t(m_t)v_2(m_t)$ ($1 + \frac{5}{3\pi}\alpha_s(m_t)$) in the $\overline{\text{DR}}$ renormalization scheme at $m_t = 175$ GeV [10], where for the evolution of the gauge couplings we use their two-loop β -functions [11]. In this way, the values of the gauge and the Yukawa couplings at M_{GUT} scale are obtained using RG equations. Then by applying these values and the remaining input parameters, λ and m_i^2 , as the boundary conditions for the RG equations at M_{GUT} scale, the numerical values of the relevant parameters at the electroweak scale are obtained through the RG evolution from M_{GUT} scale.

Appendix B

One-loop effective Higgs potential

The effective potential V_{eff} at the one-loop level may conveniently be decomposed as

$$V_{\text{eff}} = V_0 + V_b + V_t + V_g + V_s, \quad (26)$$

where V_0 denotes the tree-level potential, the equation (3), $V_b(V_t)$ the b -quark (t -quark) contribution, V_g the gauge boson contribution, and V_s the contribution of the Higgs bosons. As for V_s we first calculate the full field-dependent squared mass matrix, then omit terms containing charged Higgs fields, which do not contribute to the physical mass matrix of the Higgs bosons. Then V_s can be expressed as a sum of V_{sc} and V_{sn} , whereby V_{sc} is the contribution of the field-dependent squared mass matrix of the charged Higgs bosons, V_{sn} that of the neutral Higgs bosons. They are given by

$$\begin{aligned} V_b &= -\frac{3\mathcal{M}_b^4}{16\pi^2} \left(\log \frac{\mathcal{M}_b^2}{\mu^2} - \frac{3}{2} \right) \\ V_t &= -\frac{3\mathcal{M}_t^4}{16\pi^2} \left(\log \frac{\mathcal{M}_t^2}{\mu^2} - \frac{3}{2} \right) \\ V_g &= \frac{3\mathcal{M}_W^4}{32\pi^2} \left(\log \frac{\mathcal{M}_W^2}{\mu^2} - \frac{3}{2} \right) + \frac{3\mathcal{M}_Z^4}{16\pi^2} \left(\log \frac{\mathcal{M}_Z^2}{\mu^2} - \frac{3}{2} \right) \\ V_s &= V_{sc} + V_{sn} \\ V_{sc} &= \frac{1}{32\pi^2} \text{Str} \left[\mathcal{M}_C^2 \mathcal{M}_C^2 \left\{ \log \left(\frac{\mathcal{M}_C^2}{\mu^2} \right) - \frac{3}{2} \right\} \right] \\ V_{sn} &= \frac{\sum_{\mathcal{H}=S,P}}{64\pi^2} \text{Str} \left[\mathcal{M}_{\mathcal{H}}^2 \mathcal{M}_{\mathcal{H}}^2 \left\{ \log \left(\frac{\mathcal{M}_{\mathcal{H}}^2}{\mu^2} \right) - \frac{3}{2} \right\} \right], \end{aligned} \quad (27)$$

where μ the renormalization scale and \mathcal{M} denote the field-dependent mass matrices for the particles [7]. The Higgs doublets of the potential V_0 , the equation (3), can be defined as follows

$$H_1 = \begin{pmatrix} \frac{1}{\sqrt{2}}(S_1 + iP_1) \\ H_1^- \end{pmatrix}, \quad H_2 = \begin{pmatrix} H_2^+ \\ \frac{1}{\sqrt{2}}(S_2 + iP_2) \end{pmatrix}. \quad (28)$$

Acknowledgments

B. R. Kim was supported by the Brain Pool Program of KOSEF. He would like to thank the hospitality of CHEP, Kyungpook National University.

References

- [1] J. Wess and J. Bagger, *Supersymmetry and Supergravity*, (Princeton University Press, Princeton, 1991).
- [2] B.R. Kim, Z. Phys. **C67** (1995) 337.
- [3] S.W. Ham, B.R. Kim, G. Kreyerhoff and S.K. Oh, Phy. Lett. **B441** (1998) 215.
- [4] P. John and B.R. Kim, Z. Phys. **C73** (1996) 169.
- [5] H. Franz, B.R. Kim, and M. Weber, Eur. Phys. J. **C1** (1998) 649.
- [6] H. Franz, B.R. Kim, and M. Weber, Eur. Phys. J. **C8** (1999) 679.
- [7] D.W. Lee, B.R. Kim and S.K. Oh, J. Phys. G **30** (2004) 359.
- [8] K. Abe *et al.*, GLC Project Report (2003) 36.
- [9] Particle Data Group 2000, Eur. Phys. J. **C15** (2000) 1.
- [10] D.M. Pierce, J.A. Bagger, K.T. Matchev and Ren-Jie Zhang 1997 *Nucl. Phys. B* **491** 3.
- [11] S.P. Martin and M.T. Vaughn, Phy. Lett. **B318** (1993) 331.

Figure Captions

Fig. 1: The plot of the RG-improved mass at the one-loop level of S_1 against λ_{GUT} , for $0 \leq \lambda_{\text{GUT}} \leq 1.2$, $m_{2\text{GUT}}^2 = 0$, $0 < |m_{1\text{GUT}}^2| \text{ (TeV}^2) \leq 1$ and $0 < |m_{3\text{GUT}}^2| \text{ (TeV}^2) \leq 1$ at the GUT scale.

Fig. 2: The plot against m_{S_1} of S_1 production cross sections at the one-loop level with the RG-improved effective potential V_{eff} at future e^+e^- collider for $\sqrt{s} = 500$ GeV in the Case A.

Fig. 3: The plot against m_{S_2} and m_P of σ_{S_2} and σ_P , respectively, at the one-loop level with the RG-improved effective potential V_{eff} at future e^+e^- collider for $\sqrt{s} = 2000$ GeV in the Case A.

Fig. 4: The plot of the RG-improved mass at the one-loop level of S_1 against λ_{GUT} , for $0 \leq \lambda_{\text{GUT}} \leq 1.2$, $m_{1\text{GUT}}^2 = 0$, $0 < |m_{2\text{GUT}}^2| \text{ (TeV}^2) \leq 1$ and $0 < |m_{3\text{GUT}}^2| \text{ (TeV}^2) \leq 1$ at the GUT scale.

Fig. 5: The plot of the RG-improved mass at the one-loop level of S_2 against λ_{GUT} , for $0 \leq \lambda_{\text{GUT}} \leq 1.2$, $m_{1\text{GUT}}^2 = 0$, $0 < |m_{2\text{GUT}}^2| \text{ (TeV}^2) \leq 1$ and $0 < |m_{3\text{GUT}}^2| \text{ (TeV}^2) \leq 1$ at the GUT scale.

Fig. 6: The plot of the RG-improved mass at the one-loop level of P against λ_{GUT} , for $0 \leq \lambda_{\text{GUT}} \leq 1.2$, $m_{1\text{GUT}}^2 = 0$, $0 < |m_{2\text{GUT}}^2| \text{ (TeV}^2) \leq 1$ and $0 < |m_{3\text{GUT}}^2| \text{ (TeV}^2) \leq 1$ at the GUT scale.

Fig. 7: The plot against m_{S_1} and m_{S_2} of σ_{S_1} and σ_{S_2} , respectively, at the one-loop level with the RG-improved effective potential V_{eff} at LEP2 for $\sqrt{s} = 205.9$ GeV in the Case B.

Fig. 8: The plot of the largest σ_{S_1} for given m_{S_1} in the entire region of the parameter space at the one-loop level with the RG-improved effective potential V_{eff} at LEP2 for $\sqrt{s} = 205.9$ GeV in the Case C.

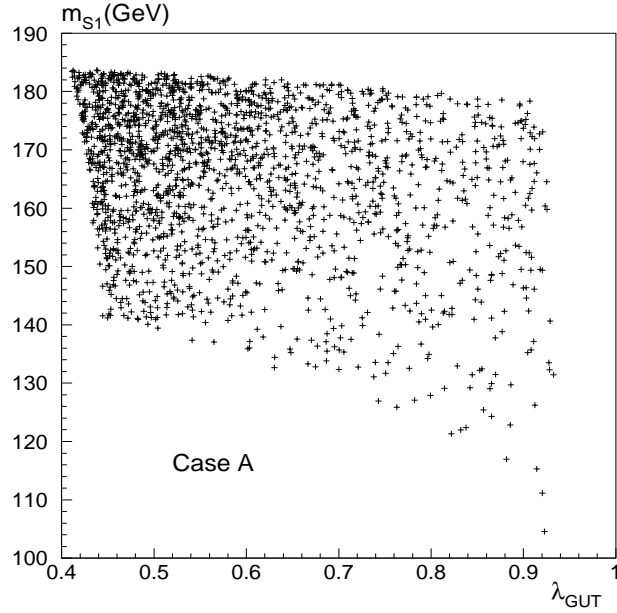


FIGURE 1: The plot of the RG-improved mass at the one-loop level of S_1 against λ_{GUT} , for $0 \leq \lambda_{\text{GUT}} \leq 1.2$, $m_{2\text{GUT}}^2 = 0$, $0 < |m_{1\text{GUT}}^2| \text{ (TeV}^2) \leq 1$ and $0 < |m_{3\text{GUT}}^2| \text{ (TeV}^2) \leq 1$ at the GUT scale.

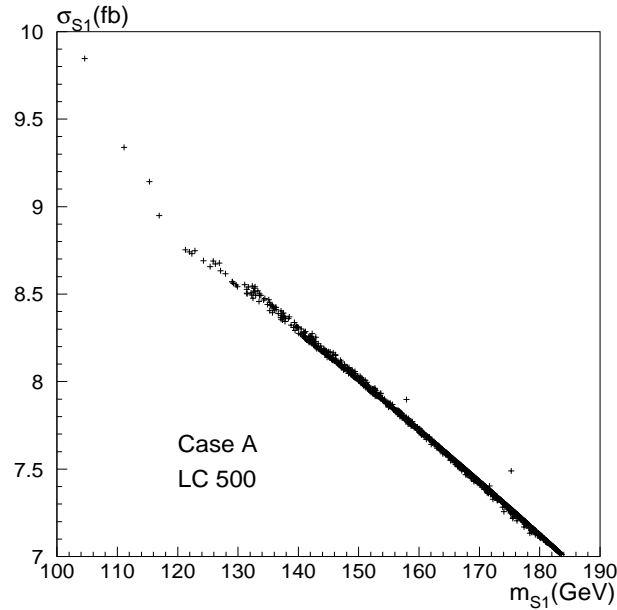


FIGURE 2: The plot against m_{S_1} of S_1 production cross sections at the one-loop level with the RG-improved effective potential V_{eff} at future e^+e^- collider for $\sqrt{s} = 500$ GeV in the Case A.

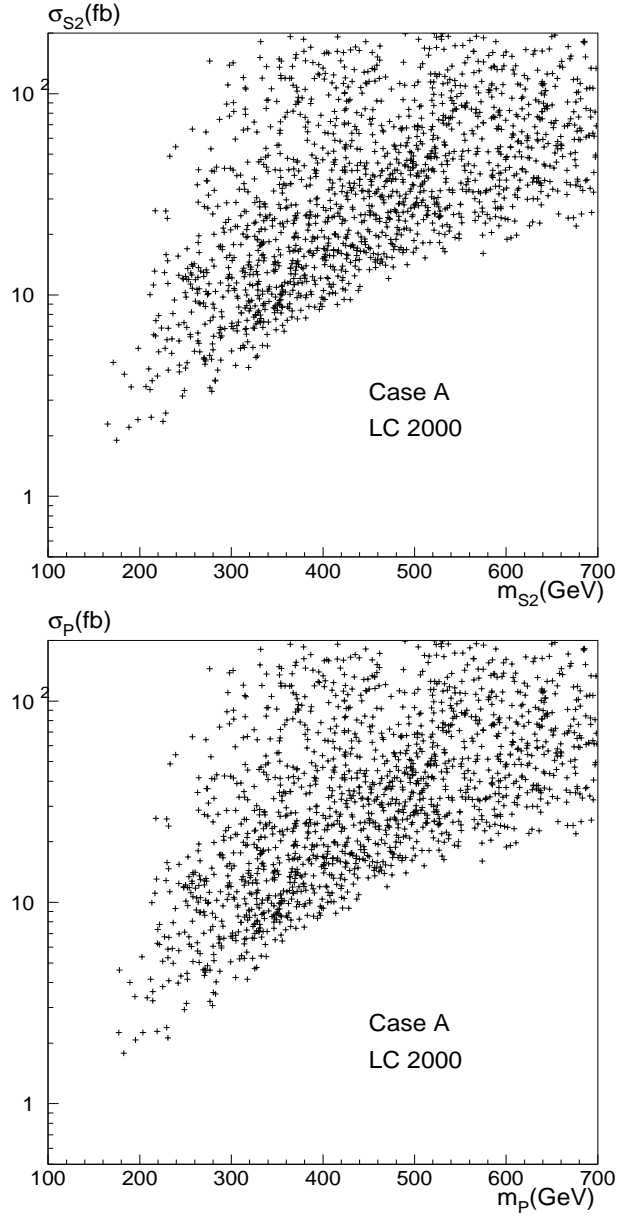


FIGURE 3: The plot against m_{S_2} and m_P of σ_{S_2} and σ_P , respectively, at the one-loop level with the RG-improved effective potential V_{eff} at future e^+e^- collider for $\sqrt{s} = 2000$ GeV in the Case A.

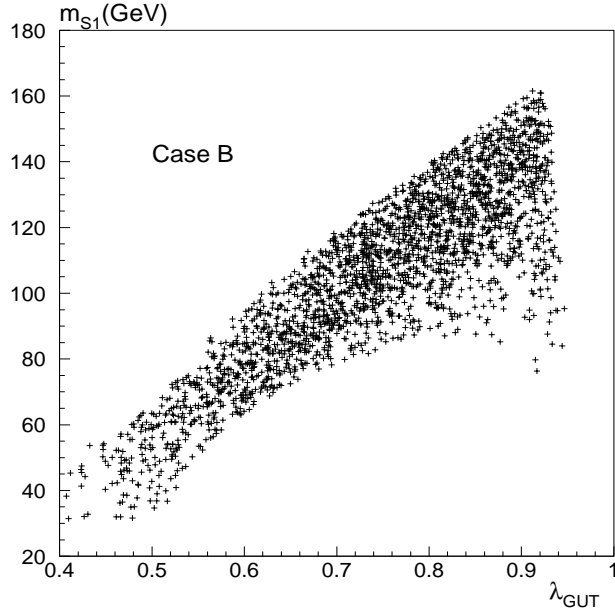


FIGURE 4: The plot of the RG-improved mass at the one-loop level of S_1 against λ_{GUT} , for $0 \leq \lambda_{\text{GUT}} \leq 1.2$, $m_{1\text{GUT}}^2 = 0$, $0 < |m_{2\text{GUT}}^2| \text{ (TeV}^2) \leq 1$ and $0 < |m_{3\text{GUT}}^2| \text{ (TeV}^2) \leq 1$ at the GUT scale.

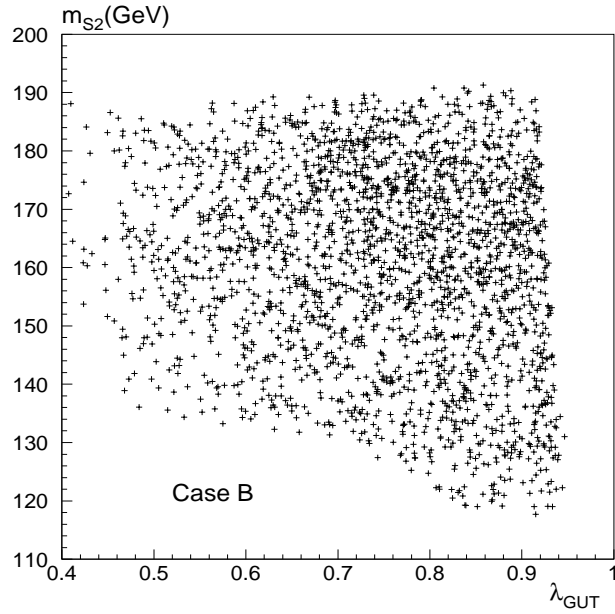


FIGURE 5: The plot of the RG-improved mass at the one-loop level of S_2 against λ_{GUT} , for $0 \leq \lambda_{\text{GUT}} \leq 1.2$, $m_{1\text{GUT}}^2 = 0$, $0 < |m_{2\text{GUT}}^2| \text{ (TeV}^2) \leq 1$ and $0 < |m_{3\text{GUT}}^2| \text{ (TeV}^2) \leq 1$ at the GUT scale.

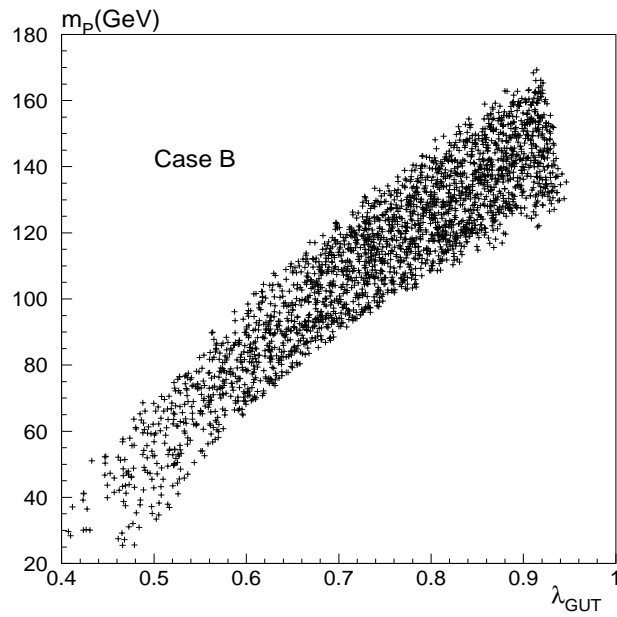


FIGURE 6: The plot of the RG-improved mass at the one-loop level of P against λ_{GUT} , for $0 \leq \lambda_{\text{GUT}} \leq 1.2$, $m_{1\text{GUT}}^2 = 0$, $0 < |m_{2\text{GUT}}^2| (\text{TeV}^2) \leq 1$ and $0 < |m_{3\text{GUT}}^2| (\text{TeV}^2) \leq 1$ at the GUT scale.

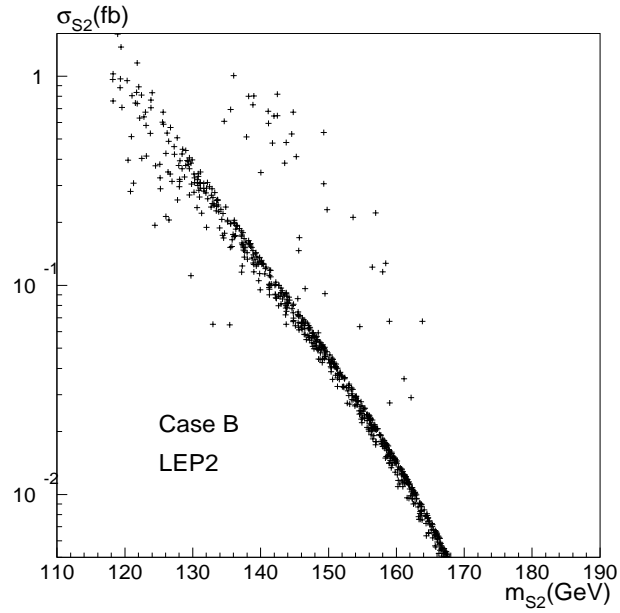
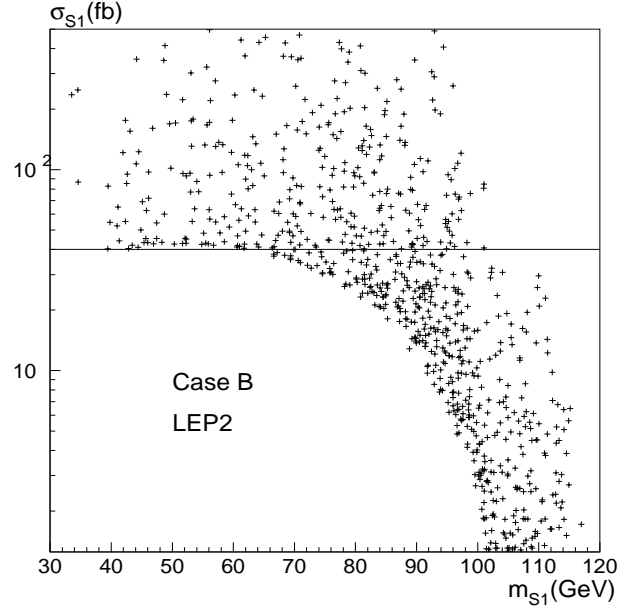


FIGURE 7: The plot against m_{S_1} and m_{S_2} of σ_{S_1} and σ_{S_2} , respectively, at the one-loop level with the RG-improved effective potential V_{eff} at LEP2 for $\sqrt{s} = 205.9$ GeV in the Case B.

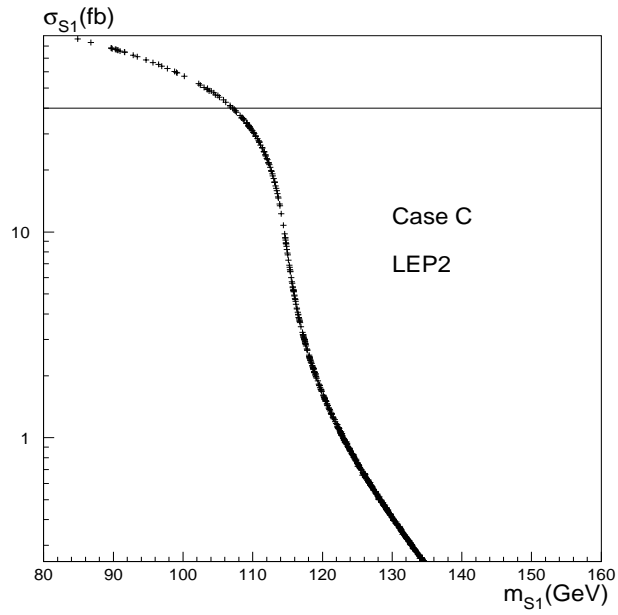


FIGURE 8: The plot of the largest σ_{S_1} for given m_{S_1} in the entire region of the parameter space at the one-loop level with the RG-improved effective potential V_{eff} at LEP2 for $\sqrt{s} = 205.9$ GeV in the Case C.